

PhysChemComm

Synthesis of CdS nanoparticles within thermally evaporated aerosol OT thin films

S. Shiv Shankar, Sayandeve Chatterjee and Murali Sastry*

Materials Chemistry Division, National Chemical Laboratory, Pune, INDIA 411 08.
E-mail: sastry@ems.ncl.res

Received 8th April 2003, Accepted 21st May 2003

First published as an Advance Article on the web 3rd June 2003

Paper

In this paper, we discuss the synthesis of cadmium sulfide (CdS) quantum dots within thermally evaporated sodium bis(2-ethylhexyl)sulfosuccinate (AOT) thin films. This procedure uses electrostatic interactions to entrap positively charged cadmium ions into thin films of the anionic surfactant AOT by a simple immersion of the film in electrolyte solution. Thereafter, the composite film is treated with H₂S gas/Na₂S solution resulting in the *in-situ* formation of CdS nanoparticles in the quantum size regime. It is believed that the ability of AOT molecules in the thermally evaporated thin films to form reverse micelles is responsible for the CdS nanoparticle size control observed. Investigation of the entrapment of cadmium ions in the AOT film and subsequent quantum dot synthesis was carried out by quartz crystal microgravimetry (QCM), UV-Vis spectroscopy, Fourier transform infrared (FTIR) spectroscopy and transmission electron microscopy (TEM) measurements.

Semiconductor nanoparticles have generated much interest due to their unique electronic,^{1–4} optical,^{5–7} catalytic^{8,9} and electrochemical¹⁰ properties compared to their bulk forms. Such behavior arises due to quantum size effects¹¹ that are manifested only in the case of particles below a certain critical size limit. Semiconductor nanoparticles that show these quantum size effects are called quantum dots. CdS nanoparticles have potential applications as optoelectronic devices,^{12,13} lasers,¹⁴ photocatalysts,¹⁵ electrochemical cells,¹⁶ fluorescent labeling of cell organelles,¹⁷ etc. These exciting applications have focused attention on the synthesis, size control and organization of nanoclusters.^{18–21} One such aspect is the formation of thin films of semiconductor nanoparticles. To realize this, procedures such as the Langmuir–Blodgett technique^{22–26} and liquid–liquid interface reaction technique²⁷ have been developed. Electrostatic interactions help cadmium ions from the sub-phase complex with the anionic surfactant molecules. Subsequently, the films, after lifting onto a suitable substrate, are treated with Na₂S solution for synthesis of CdS nanoparticles.

In this laboratory, some of us have successfully used electrostatic interactions to entrap cadmium ions into thermally evaporated fatty acid films and then form CdS nanoparticles by chemical treatment of the immobilized cadmium ions.²⁸ In the present work, we describe attempts to synthesize cadmium sulfide nanoparticles within thermally evaporated thin films of sodium bis(2-ethylhexyl)sulfosuccinate (AOT). The choice of AOT was motivated by the possibility of better size control over formation of CdS nanoparticles. AOT, a well-known capping agent for semiconductor nanoparticles, is a double-chain anionic surfactant. Their tendency to form spherical reverse micelles whose size increases with increase in W_o (the molar ratio of water to surfactant in oil)²⁹ has been used with success in the synthesis of inorganic nanoparticles of controlled dimensions. Though the conditions of our experiment are not identical to that experienced by AOT in reverse micelles, we believe that the propensity of this surfactant to form spherical structures in an aqueous environment would provide a confining influence on CdS nanoparticles formed in the AOT matrix and thus, better control over nanoparticle size than that afforded by stearic acid thin films.²⁸ Another motivating factor for the use of AOT is the interesting optical properties of AOT

capped CdS nanoparticles.^{30–33} Synthesizing nanoparticles such as CdS in lipid thin films by electrostatic entrapment of suitable ions can potentially provide many additional advantages over other methods of forming nanoparticulate thin films. Using this method it is possible to achieve patterned nanoparticulate thin films by suitable masking of the lipid film. Apart from allowing the possibility of pattern formation, our method enables the convenient formation of nanoparticulate thin films even on nonplanar and topologically highly complex surfaces, which is difficult if not impossible to achieve by other thin film forming techniques. By sequential entrapment of different metal ions, formation of nanocomposite thin films constituted by different semiconducting nanoparticles or formation of doped semiconducting nanoparticulate thin film should also be achievable. As a first step in this direction, the present communication focuses on the synthesis of CdS nanoparticles in thin films of aerosol OT. Presented below are details of the investigation.

Thin films of AOT of 500 Å thickness were thermally vacuum deposited in an Edwards E306A vacuum coating unit at a pressure better than 1×10^{-7} Torr onto glass, Si (111) wafers, carbon-coated copper transmission electron microscopy (TEM) grids and gold-coated AT-cut quartz crystals [for quartz crystal microgravimetry (QCM) measurements]. In our present work Cd²⁺ ions were entrapped in 500 Å AOT thin films by simple immersion of the thin film coated substrate into CdSO₄ solution. The driving force for the entrapment is the attractive electrostatic interactions between the cadmium cations present in the solution and the anionic sulfate group of AOT molecules within the thin film matrix. Entrapment of Cd²⁺ ions in AOT film and its subsequent treatment with S²⁻ ions by immersion in Na₂S solution was monitored by *ex-situ* QCM measurements using an Edwards FTM5 frequency counter after thorough washing and drying of the QCM crystals prior to measurement. Conversion of the QCM frequency change to mass loading was done using the standard Sauerbrey equation³⁴ to estimate the net intake of cadmium ions into the AOT matrix. Fig. 1A shows the QCM kinetics data for the mass uptake by the AOT film during immersion in the CdCl₂ solution at regular intervals. From the equilibrium mass loading of the cadmium ions (48 μg cm⁻²) in the thin film

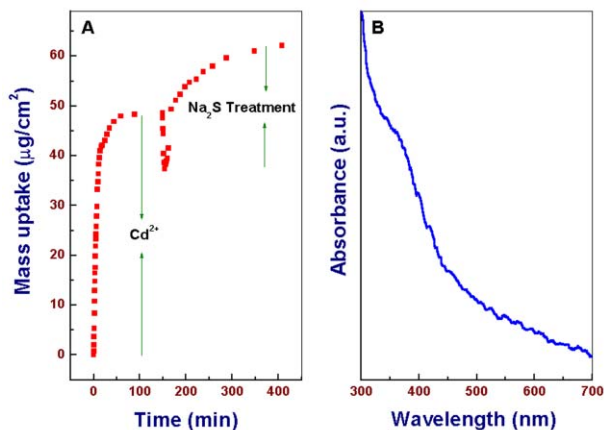


Fig. 1 (A) Quartz crystal microgravimetry measurements of the Cd^{2+} mass intake in a 500 Å thick AOT film as a function of time of immersion in the CdCl_2 solution and thereafter, reaction with sulfide ions by immersion in Na_2S solution. (B) UV-Vis absorption spectrum of CdS nanoparticles synthesized within a 500 Å thick AOT film deposited on a quartz substrate.

and the knowledge of the AOT mass deposited initially, an AOT : Cd^{2+} molar ratio of 1 : 42 was calculated. The above observation clearly indicates considerable overcompensation of the negative charge due to the sulfate groups in the AOT matrix by the Cd^{2+} ions. Such charge overcompensation (though not to this extent) is known to occur in the layer-by-layer electrostatically assembled systems.³⁵ This ‘apparently’ large charge overcompensation could also be due to a large change in the acoustic properties of the AOT film consequent to Cd^{2+} entrapment. During the next cycle of treatment of the cadmium sulfosuccinate film in Na_2S solution for the formation of CdS nanoparticles (Fig. 1A), it is observed that there is an initial decrease in mass of the film. The mass change in the film reaches a minimum after approximately 5 min of immersion with a *ca.* mass loss of $10.17 \mu\text{g cm}^{-2}$ observed. This fall in mass is followed by an increase giving a subsequent mass uptake of *ca.* $24.77 \mu\text{g cm}^{-2}$ after 6 h of immersion leading to a net mass uptake of $14.7 \mu\text{g cm}^{-2}$ relative to the Cd^{2+} ions entrapped AOT film. A number of factors could be responsible for the observed trends in mass change. The initial mass loss could be due to partial leaching out of the cadmium ions from the AOT film. The mass increase observed thereafter could be explained on the basis that during formation of CdS, an uncharged entity, fresh sulfonate groups are regenerated leading to the possibility of complexation of positively charged Na^+ ions within the film. Another possible contributing factor for the observed mass increase could be a large change in the acoustic properties of the composite nanoparticulate thin film of AOT with entrapped semiconducting nanoparticles. The changes in the acoustic properties could originate from a considerable change in the viscoelastic behavior during formation of CdS nanoparticles. The contribution from the change in acoustic properties to the observed mass change has not been taken into account in the analysis both during immersion in CdCl_2 solution and during treatment with Na_2S solution. We are pursuing this aspect currently.

Entrapment of Cd^{2+} ions in the AOT film was followed by immersion of the cadmium sulfosuccinate film in Na_2S solution for the formation of CdS nanoparticles. To the naked eye, the film exhibited a yellowish tinge following Na_2S treatment clearly indicating the formation of CdS nanoparticles. Fig. 1B shows the UV-Vis spectrum recorded from the 500 Å thick film after the treatment with S^{2-} ions. From the UV-Vis absorption spectrum, it is seen that an absorption band with an onset of absorption located at *ca.* 413 nm occurs in the chemically treated cadmium sulfosuccinate thin film. This absorption edge

is blue-shifted relative to bulk form of CdS, which is known to occur at 510 nm. The blue-shift in the absorption edge observed here with AOT thin films is an indicator that the CdS nanoparticles formed within the AOT matrix are in the quantum dot regime. An estimate of the CdS nanoparticle size may be made from the following equation obtained by Brus¹¹ for the lowest direct interband transition energy of a spherical quantum dot of radius R_0 in the effective mass approximation:

$$E(R_0) = E_0 + \frac{\hbar^2 \pi^2}{2} \left(\frac{1}{m_e} + \frac{1}{m_h} \right) \frac{1}{R_0^2} - \frac{1.8e^2}{\epsilon R_0} + \frac{e^2}{R_0} \sum_{n=1}^{\infty} \alpha_n \left(\frac{S}{R_0} \right)^{2n}$$

where E_0 is the band gap in the bulk form, m_e and m_h are the effective mass of electrons and holes respectively, e the electronic charge, ϵ the dielectric constant of the medium and α_n is a function of dielectric constants and S is the electron-hole separation. The second term in the right hand side of the above equation represents the quantum localization energy. The third and fourth terms correspond to the Coulomb potential and polarization energy respectively. For nanoparticles of CdS with radius in the range 1 to 4 nm, the polarization term is typically one third of the Coulomb term with opposite sign.¹¹ Incorporation of correction for the polarization term by appropriately rescaling the coefficient of the coulomb term leads to the following simplified expression for the energy $E(R)$ for CdS particles of radius R , $E_0 = 2.43 \text{ eV}$ and $\epsilon = 5.7$.

$$E(R) = 2.43 + \frac{2.446}{R^2} - \frac{0.3031}{R}$$

From the above equation, the radius of the CdS quantum dots synthesized within the AOT thin films was estimated to be 1.8 nm. We would like to emphasize here that the size of the CdS nanoparticles grown in AOT thin films is significantly smaller than that observed in our earlier study on CdS growth in thermally evaporated stearic acid films where the absorption band edge was observed at 470 nm.²⁸

FTIR measurements for the AOT thin film of thickness 500 Å were done at each stage of treatment to study the complexation of the Cd^{2+} ions to the AOT molecules after immersion in CdSO_4 solution and after treatment with S^{2-} ions for CdS nanoparticle synthesis. The spectrum corresponding to a pure AOT thin film represented as curve 1 in Fig. 2A showed peaks at 1160 and 1052 cm^{-1} corresponding to asymmetric and symmetric stretch vibrations of the sulfonate groups and at 1247 cm^{-1} , which corresponds to the ester stretch ($-\text{C}(=\text{O})-\text{O}-\text{C}$).³⁶ A shift in the S–O stretching frequency from 1160 to 1113 cm^{-1}

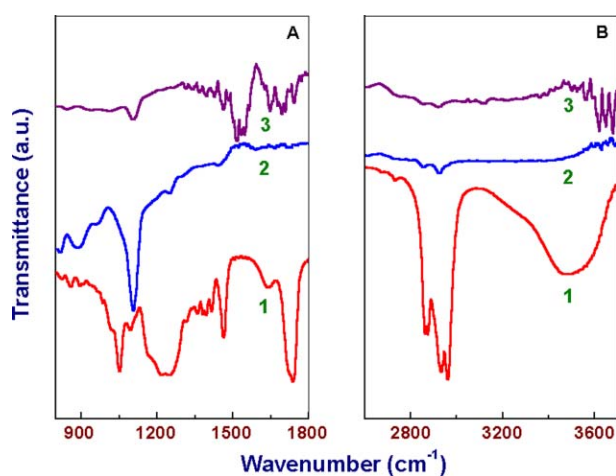


Fig. 2 (A) and (B): FTIR spectra recorded from a 500 Å thick AOT film (curve 1) on a Si (111) wafer, the AOT film shown as curve 2 after entrapment of Cd^{2+} ions and the Cd-AOT film shown as curve 3 in two different spectral windows (see text for details).

was observed in the AOT film after immersion in CdCl_2 solution (curve 2, Fig. 2A). After formation of CdS (curve 3, Fig. 2A), there is no further shift in the peak value corresponding to the S–O stretching vibrational mode indicating that the AOT molecules are still bound to the cadmium ions on the surface of the CdS nanocrystals or could possibly be due to the presence of Na^+ ions as discussed above in relation to the observed QCM mass change. The intense peaks at 2854 and 2924 cm^{-1} corresponding to methylene antisymmetric and symmetric vibrational modes in AOT (curve 1) as shown in Fig. 2B are reduced in intensity after incorporation of Cd^{2+} ions (curve 2) and further reduced after formation of CdS (curve 3) indicating randomization in the orientation of the hydrocarbon chains consequent to ion entrapment.

The elemental composition of the composite CdS–AOT thin film was determined using energy dispersive analysis of X-rays (EDAX). The EDAX spectrum recorded from a 500 \AA thick AOT film after formation of CdS nanoparticles is shown in Fig. 3. A quantitative analysis of the film revealed that the atomic ratio of Cd and S in the film was *ca.* 1 : 2.2. It should be noted here that the contribution of the S atoms in the EDAX spectrum comes from both S atoms present in the AOT molecules and from those in the CdS nanoparticles and would explain the larger than unity molar ratio of sulfur relative to cadmium.

Fig. 4 shows a low magnification TEM image of CdS nanoparticles formed in a 500 \AA thick AOT thin film as described earlier. While an exact estimate of the particle size cannot be made from this image, it is clear that the CdS nanoparticles are formed at sufficiently high density within the AOT film. A better idea of the particle size and shape may be had from the high magnification TEM picture of the CdS nano-AOT composite film shown in Fig. 4A. From this picture, it is clearly seen that the particles are essentially spherical and fairly monodisperse. Fig. 5B shows the particle size distribution histogram measured from a number of CdS nanoparticles shown in Fig. 5A and other similar micrographs. From a Gaussian fit to the histogram (solid line, Fig. 5B), an average CdS nanoparticle size $3 \pm 0.6\text{ nm}$ was estimated.

From XRD measurements, it was concluded that the particles are hexagonal CdS nanocrystals. XRD measurement of the AOT thin film after incorporation of Cd^{2+} ions showed no lamellar ordering which is commonly observed in case of stearic acid or octadecyl amine.³⁷ Unlike AOT having double hydrocarbon chains, stearic acid and octadecyl amine molecules are single chained molecules and tend to pack in planar

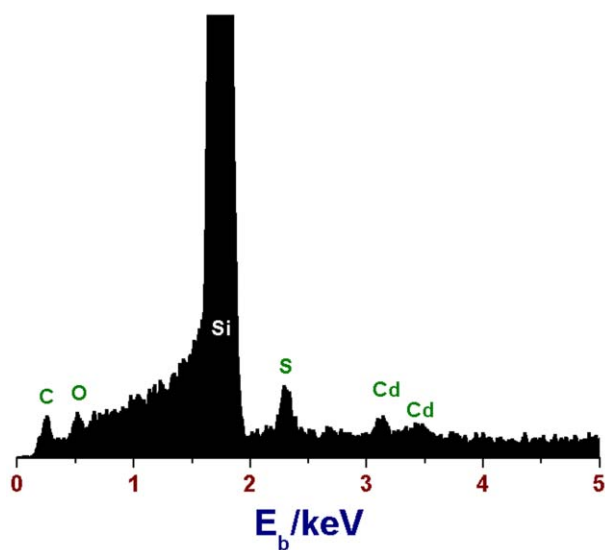


Fig. 3 EDAX spectrum showing the presence of cadmium and sulfur in a 500 \AA thick composite CdS nano-AOT thin film.

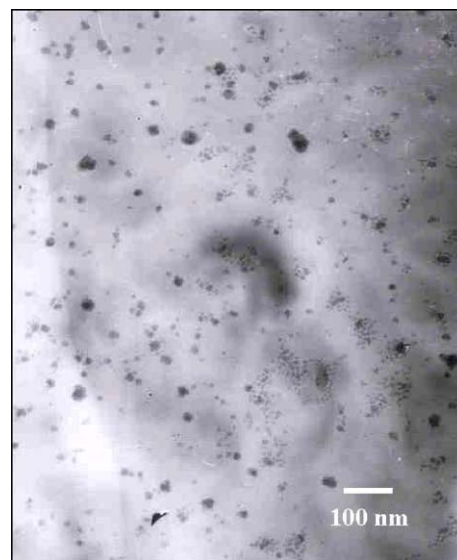


Fig. 4 Low magnification TEM picture of CdS nanoparticles formed in a 500 \AA thick thermally evaporated AOT film deposited on a carbon-coated copper TEM grid.

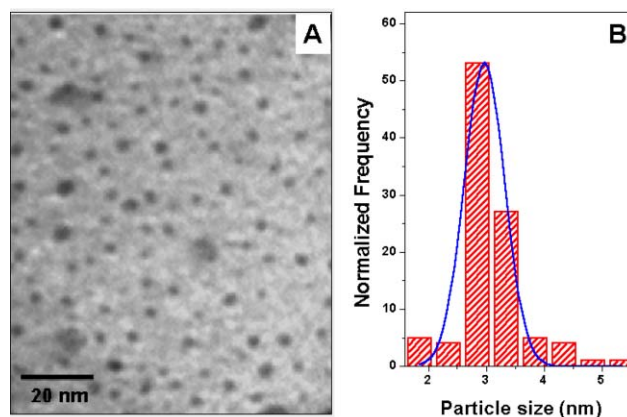


Fig. 5 (A) Representative TEM micrograph and, (B) particle size distribution histogram of CdS nanoparticles formed in a 500 \AA thick thermally evaporated AOT film deposited on a carbon-coated copper TEM grid. The solid line in B is a Gaussian fit to the particle size distribution histogram.

structures in the form of bilayer stacks.³⁷ AOT as mentioned above has an inherent tendency to form spherical reverse micelles. Perhaps due to this nature, AOT is able to inhibit the growth of the CdS nanoparticle and thus help in forming quantum dots with a better size control.

In conclusion CdS nanoparticles have been synthesized within thermally evaporated thin films of aerosol OT by electrostatic entrapment of Cd^{2+} ions and their subsequent treatment with Na_2S . This technique shows promise for the realization of patterned structures of nanoparticulate CdS thin films as well as doped CdS nanoparticles to improve the optoelectronic properties of these composite films.

References

1. A. Henglein, *Chem. Rev.*, 1989, **89**, 1861.
2. M. L. Steigerwald and L. E. Brus, *Acc. Chem. Res.*, 1990, **23**, 183.
3. Y. Wang and N. Herron, *J. Phys. Chem.*, 1991, **95**, 525.
4. H. Weller, *Angew. Chem., Int. Ed. Engl.*, 1993, **32**, 41.
5. Y. Wang, *Acc. Chem. Res.*, 1991, **24**, 133.
6. E. Rosencher, A. Fiore, B. Vinter, V. Berger, P. Bois and J. Nagle, *Science*, 1996, **271**, 168.
7. M. A. Hines and P. Guyot-Sionnest, *J. Phys. Chem. B*, 1996, **100**, 468.
8. A. J. Bard, *Science*, 1980, **207**, 4427.

- 9 S. Yanagida, M. Yooshiya, T. Shiragami, C. J. Pac, H. Mori and H. Fujita, *J. Phys. Chem.*, 1990, **94**, 3104.
- 10 S. K. Haram, B. M. Quinn and A. J. Bard, *J. Am. Chem. Soc.*, 2001, **123**, 8860.
- 11 L. E. Brus, *J. Chem. Phys.*, 1984, **80**, 4403.
- 12 V. L. Colvin, M. C. Schlamp and A. P. Alivisatos, *Nature*, 1994, **370**, 354.
- 13 B. O. Dabbousi, M. G. Bawendi and O. Onitsuka, *Appl. Phys. Lett.*, 1995, **66**, 1316.
- 14 L. Pavesi, L. D. Negro, C. Mazzoleni, G. Franzo and F. Priolo, *Nature*, 2000, **408**, 440.
- 15 C. K. Graetzel and M. Graetzel, *J. Am. Chem. Soc.*, 1979, **101**, 7741.
- 16 A. Hagfeldt and M. Graetzel, *Chem. Rev.*, 1995, **95**, 49.
- 17 Jr M. Bruchez, M. Moronne, P. Gin, S. Weiss and A. P. Alivisatos, *Science*, 1998, **281**, 2013.
- 18 P. V. Braun, P. Osenar and S. I. Stupp, *Nature*, 1996, **380**, 325.
- 19 H. Weller, *Angew. Chem., Int. Ed. Engl.*, 1993, **32**, 41.
- 20 J. H. Fendler, *Curr. Opin. Colloid Interface Sci.*, 1996, **1**, 202.
- 21 N. Kimizuka and T. Kunitake, *Adv. Mater.*, 1996, **8**, 89.
- 22 A. V. Nabok, A. K. Ray, A. K. Hassan, J. M. Titchmarsh, F. Davis, T. Richardson, A. Starovoitov and S. Bayliss, *Mater. Sci. Eng., C*, 1999, **8-9**, 171.
- 23 C. Damle, A. Gole and M. Sastry, *J. Mater. Chem.*, 2000, **10**, 1389.
- 24 G. Hemakanthi, B. U. Nair and A. Dhathathreyan, *Proc. Indian Acad. Sci., Chem. Sci.*, 2000, **112**, 109.
- 25 S. Guo, L. Konopny, R. Popowitz-Biro, H. Cohen, H. Porteanu, E. Lifshitz and M. Lahav, *J. Am. Chem. Soc.*, 1999, **121**, 9589.
- 26 H. Bekele, J. H. Fendler and J. W. Kelly, *J. Am. Chem. Soc.*, 1999, **121**, 7266.
- 27 S. D. Sathaye, K. R. Patil, D. V. Paranjape, A. Mitra, S. V. Awate and A. B. Mandale, *Langmuir*, 2000, **16**, 3487.
- 28 S. Mandal, C. Damle, S. R. Sainkar and M. Sastry, *J. Nanosci. Nanotech.*, 2001, **1**, 281.
- 29 E. Ruckenstein and R. Nagarajan, *J. Phys. Chem.*, 1980, **84**, 1349.
- 30 M. Meyer, C. Wallberg, K. Kurihara and J. Fendler, *J. Chem. Soc., Chem. Commun.*, 1984, 90.
- 31 Y. Zhang, D. Fu, X. Wang, L. Juzheng and L. Zuhong, *Colloids Surf., A*, 2001, **181**, 145.
- 32 D. Fu, M. Li, X. Wang, J. Cheng, Y. Zhang, Z. Lu and J. L. Cui, *Supramol. Sci.*, 1998, **5**, 495.
- 33 M. Tata, S. Banerjee, V. T. John, Y. Waguespack and G. L. McPherson, *Colloids Surf., A*, 1997, **127**, 39.
- 34 G. Saurbrey, *Z. Phys.*, 1959, **155**, 206.
- 35 N. Cu villier and F. Rondelez, *Thin Solid Films*, 1998, **327-329**, 19.
- 36 N. Takuya, O. Bunsho and U. Kohei, *J. Phys. Chem. B*, 1998, **102**, 1571.
- 37 P. Ganguly, S. Pal, M. Sastry and M. N. Shashikala, *Langmuir*, 1995, **11**, 1078.